Effect of minor addition on dynamic mechanical relaxation in ZrCu-based metallic glasses

Y.T. Cheng[a], Q. Hao[a], J.C. Qiao[a,*], D. Crespo[b], E. Pineda[b,*], J.M. Pelletier[c]

[a]*School of Mechanics, Civil Engineering and Architecture, Northwestern Polytechnical University, Xi'an 710072, China*

[b]*Departament de Física, Centre de Recerca en Ciència i Enginyeria Multiescala de Barcelona, Institut de Tècniques Energètiques, Universitat Politècnica de Catalunya, 08019 Barcelona, Spain*

[c]*Université de Lyon, MATEIS, UMR CNRS5510, Bat. B. Pascal, INSA-Lyon, F-69621 Villeurbanne cedex, France*

*Corresponding author: qjczy@nwpu.edu.cn (Dr. J.C. Qiao)

eloi.pineda@upc.edu (Dr. E. Pineda)

Abstract: The dynamic mechanical behavior of $Zr_{50-x}Cu_{34}Ag_8Al_8Pd_x$ (x = 0 and 2) bulk metallic glasses was probed by mechanical spectroscopy. The results suggest that microalloying retards the relaxation dynamics. The physical aging was analyzed considering a model based on the variation of the concentration of flow units and the Kohlrausch-Williams-Watts (KWW) equation. In the current study, the characteristic parameters of the two models, β_c and β_{aging}, reflect the faster annihilation of flow units at higher temperature and the increase of dynamic heterogeneity with temperature, respectively. The mechanical relaxation spectrum was also analyzed. Based on the KWW equation and QPD model, replacing Zr with a small amount of Pd can slightly increase the dynamic inhomogeneity and reduce the defect concentration. The analysis according to the HN function suggests that the addition of Pd increases the relaxation time. However, it does not significantly alter the shape of the relaxation time distribution.

Keywords: Metallic glass; Mechanical relaxation; Structural heterogeneity; Physical model

1. Introduction

Compared with their conventional crystalline counterparts, metallic glasses show promising mechanical properties such as high specific strength, high fracture toughness and large elastic deformation capacity[1-3]. In addition, metallic glasses may show excellent corrosion resistance[4]. The essential properties of metallic glasses are the exceptional shaping ability in the supercooled liquid region (SLR)[5, 6] and the possibility to apply low-temperature forming[7], the latter process critically dependent on the structural relaxation (or physical aging) behavior. Many investigations have demonstrated that metallic glasses are potential engineering materials and functional materials[4, 8]. The unusual mechanical and rheological properties among metals, coming from their disordered structure, open many possibilities to use these materials in new advanced manufacturing processes[9] provided the mechanical relaxation behavior is known in detail.

As a newcomers to the glass family, metallic glasses present complex mechanical relaxation processes still not well understood[10]. Previous work revealed that mechanical relaxation processes are essential to understand the mechanical, physical and thermal properties of amorphous solids[11-14]. The main relaxation process in glasses is called primary or α relaxation, and it is observed as the temperature is increased approaching the supercooled liquid region. It is well documented that α relaxation is a global, structural atomic/molecular reordering process, which is active above the glass transition phenomenon measured by differential scanning calorimetry (DSC)[11, 15]. Below the glass transition temperature T_g, secondary relaxations (including fast and slow β relaxations) decouple from α relaxation[7, 16]. It is believed that secondary relaxation is closely connected to the structural heterogeneity of metallic glasses[17]. Notably, the secondary relaxation process is linked to the mechanical properties (i.e. plasticity)[16, 18], diffusivity[11] and glass transition behavior[7] of metallic glasses. Intense research about these topics is now undergoing, and many questions are still under discussion[7, 17, 19-21].

Mechanical relaxation behavior is strongly dependent on the chemical composition

and physical aging below the glass transition temperature[22, 23]. According to mechanical spectroscopy, in general, La-based metallic glasses show an intense slow β relaxation process displaying a prominent peak in their loss modulus E''[24], Pd-based metallic glasses exhibit a "shoulder" in E''[15] and Zr-based metallic glasses display the so-called "excess wing" in E''[25]. The slow β relaxation is sensitive to physical aging, and it is suggested that it is associated with the structural heterogeneity, i.e. structural "defects" such as flowing units[26], quasi-point defects[27, 28] or soft and hard regions[29, 30]. Through physical aging the concentration of "defects" could be changed[31]. As a consequence, the intensity of the slow β relaxation decreases after aging.

In parallel, micro-alloying is an effective way to tune the dynamic relaxation process and mechanical properties of metallic glasses[32-36]. For instance, the strength of β-relaxation in $(Cu_{0.5}Zr_{0.5})_{100-x}Al_x$ metallic glass is modified by introducing Al[32] and in $Cu_{36}Zr_{47-x}Al_7Dy_x$ metallic glass is decreased with increasing Dy content[33]. Microalloying is known to have also an effect on toughness, either negative[34] or positive[36], and ductility can also be enhanced[33, 35]. Micro-alloying has a complex impact on metallic glasses; therefore, understanding and controlling it is a key factor in designing and employing new metallic glasses.

In the current research, the dynamic mechanical relaxation behavior of typical Zr-based metallic glasses was probed by dynamic mechanical analysis (DMA). The effect of minor addition of Pd on $Zr_{50}Cu_{34}Ag_8Al_8$ metallic glass on the relaxation dynamics was analyzed in the framework of different models.

2. Experimental procedure

In the current work, $Zr_{50-x}Cu_{34}Ag_8Al_8Pd_x$ (x = 0 and 2) metallic glasses were prepared in an Ar atmosphere by arc-melting technique. In order to ensure the chemical uniformity of master alloys, each alloy ingot was re-melted four times at least. Plate samples with a length of 85 mm, width of 10 mm and thickness of 2 mm were obtained using copper mold suction casting. The glassy nature of the alloys in as-cast state and after thermal treatment was verified by X-ray diffraction (XRD, Philips PW3830) at ambient temperature. The scanning angle in XRD experiment ranges from 20° to 90°.

The thermal properties of metallic glasses were characterized by differential scanning calorimetry (DSC, NEZTCH 404 C). DSC tests were performed under a high-purity dry nitrogen atmosphere at a heating rate of 10 K/min.

The mechanical relaxation behavior of metallic glasses was investigated by dynamic mechanical analysis using a commercial device (DMA Q800, TA, USA) and an inverted torsion instrument with a high vacuum environment in INSA Lyon, France[37]. Plate samples were cut into 30 mm (length) × 2 mm (width) × 1 mm (height). The strain ε of the samples can be measured under a sinusoidal stress σ by DMA, where $\sigma = \sigma_0 \sin(\omega t)$ ($\omega = 2\pi f$, where ω is the angular frequency and f is the frequency) and $\varepsilon = \varepsilon_0 \cos(\omega t + \delta)$ (δ is the phase lag). Complex Young modulus, $E^* = E' + iE''$, and shear modulus, $G^* = G' + G''$, can be deduced from σ/ε. Two measurement modes were used in the current study: (I) Isochronal tests of metallic glasses were carried out on the DMA Q800 device under single cantilever mode with a constant heating rate at a given frequency. (II) Isothermal measurements were carried out on the inverted torsion instrument probing a frequency range from 0.01 to 2 Hz. Isothermal measurements were performed at intervals of 5 K.

3. Results and discussion

3.1. X-ray diffraction analysis and thermal properties of the metallic glasses

The XRD patterns of $Zr_{50-x}Cu_{34}Ag_8Al_8$ Pd_x (x = 0 and 2) metallic glasses are shown in **Fig. 1**(a); both alloys exhibit typical broad diffraction humps without any crystalline peak, confirming their amorphous structure. **Fig. 1**(b) presents the DSC curves of $Zr_{50}Cu_{34}Ag_8Al_8$ and $Zr_{48}Cu_{34}Ag_8Al_8Pd_2$ metallic glasses at a constant heating rate of 10 K/min. The addition of Pd increases the glass transition temperature T_g of the alloy from 670 K to 679 K, as indicated in the figure.

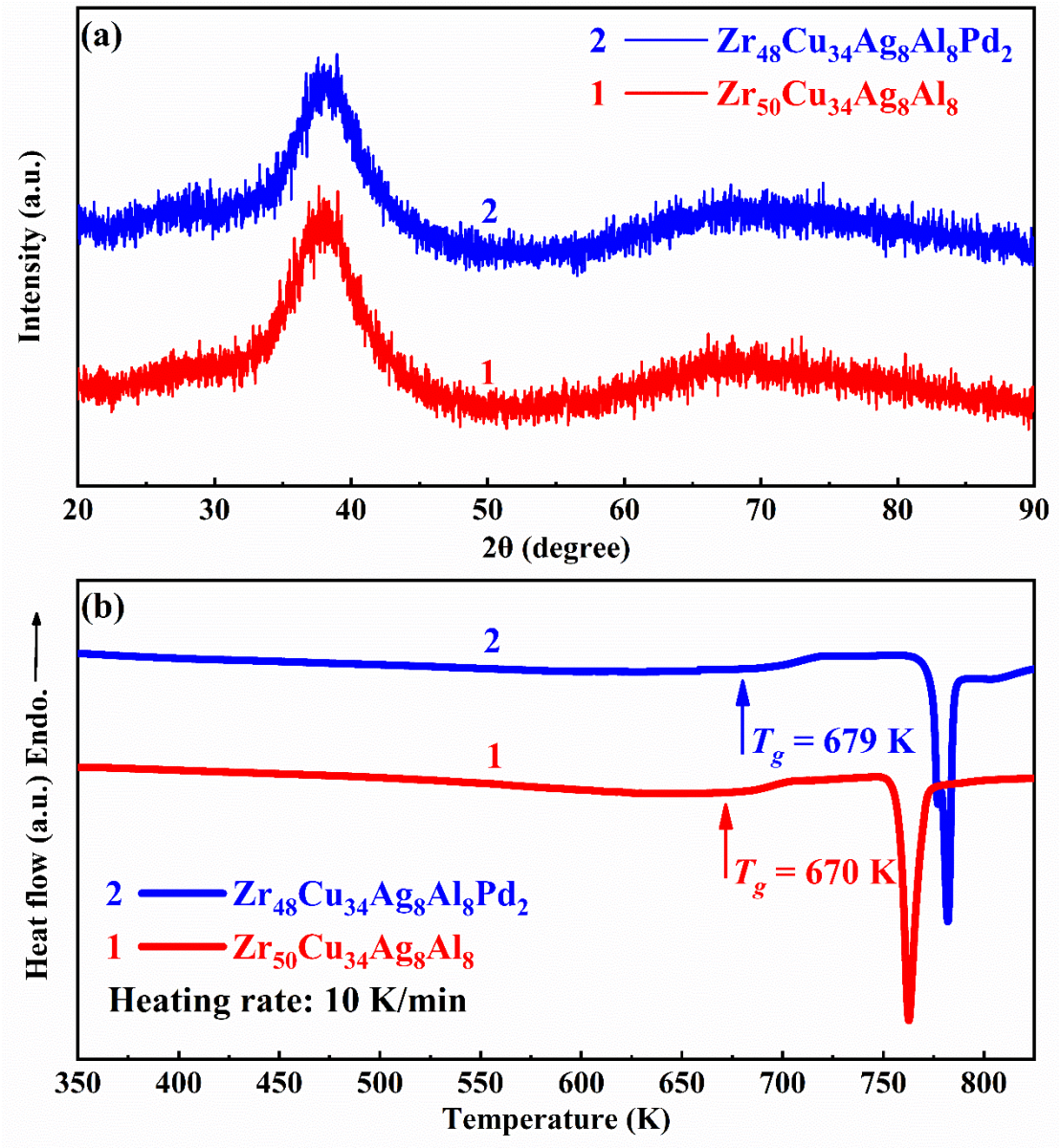

Fig. 1 (a) XRD patterns of $Zr_{50}Cu_{34}Ag_8Al_8$ and $Zr_{48}Cu_{34}Ag_8Al_8Pd_2$ metallic glasses. (b) DSC curves of the $Zr_{50}Cu_{34}Ag_8Al_8$ and $Zr_{48}Cu_{34}Ag_8Al_8Pd_2$ metallic glasses at a heating rate of 10 K/min. The arrows in Fig. 1(b) denote the temperatures of the onset of the corresponding glass transition T_g.

3.2. Mechanical relaxation behavior of metallic glasses

3.2.1. Isochronal analyses

The dynamic mechanical response of the alloys was recorded from ambient temperature to 823 K to characterize the relaxation processes. The driving frequency was 1 Hz and the heating rate 3 K/min. **Fig. 2**(a) shows the normalized storage modulus

E'/E_u, the normalized loss modulus E''/E_u and the loss factor tanδ of the $Zr_{48}Cu_{34}Ag_8Al_8Pd_2$ metallic glass. E_u is the unrelaxed modulus at room temperature. The loss factor, $\tan\delta = E''/E'$, is related to the atomic or molecular mobility of glassy materials [38].

Based on **Fig. 2**(a), the mechanical relaxation behavior of $Zr_{48}Cu_{34}Ag_8Al_8Pd_2$ metallic glass can be divided into three distinct regions: (I) For temperatures below 650 K the storage modulus is high and nearly constant while the loss modulus is very low. The metallic glass stays in the elastic deformation region. (II) In the temperature range from 650 K to 770 K, the storage modulus decreases while loss modulus increases. The loss modulus reaches its maximum around 715 K as a consequence of the α relaxation process, which is linked to the cooperative movement of the atoms [39]. (III) Above 770 K both storage modulus and loss modulus increase with temperature due to the nucleation and growth of crystalline phases.

Micro-alloying is an effective way to tune mechanical and physical properties in metallic glasses[32-36]. In the current work, Palladium (Pd) was used to replace Zr in the model alloy $Zr_{50}Cu_{34}Ag_8Al_8$. According to a previous publication[40], plasticity is enhanced by replacing Zr with Pd in $Zr_{50}Cu_{34}Ag_8Al_8$ metallic glass. **Fig. 2**(b) shows the loss factor of both alloys as a function of temperature. The loss factor decreases by the minor addition of Pd in CuZr-based metallic glass. In addition, the peak of the loss factor moves to a higher temperature, which agrees with the exothermic peak of the DSC curve moving to higher temperature in **Fig. 1**(b). The result is in line with previous reports that microalloying retards the relaxation process, for instance, the strength of β-relaxation was decreased by microalloying in refs.[32, 33]. Analogously, atomic mobility was hindered by introducing Ti in a Zr-based metallic glass, resulting in a decrease of the loss factor peak[41].

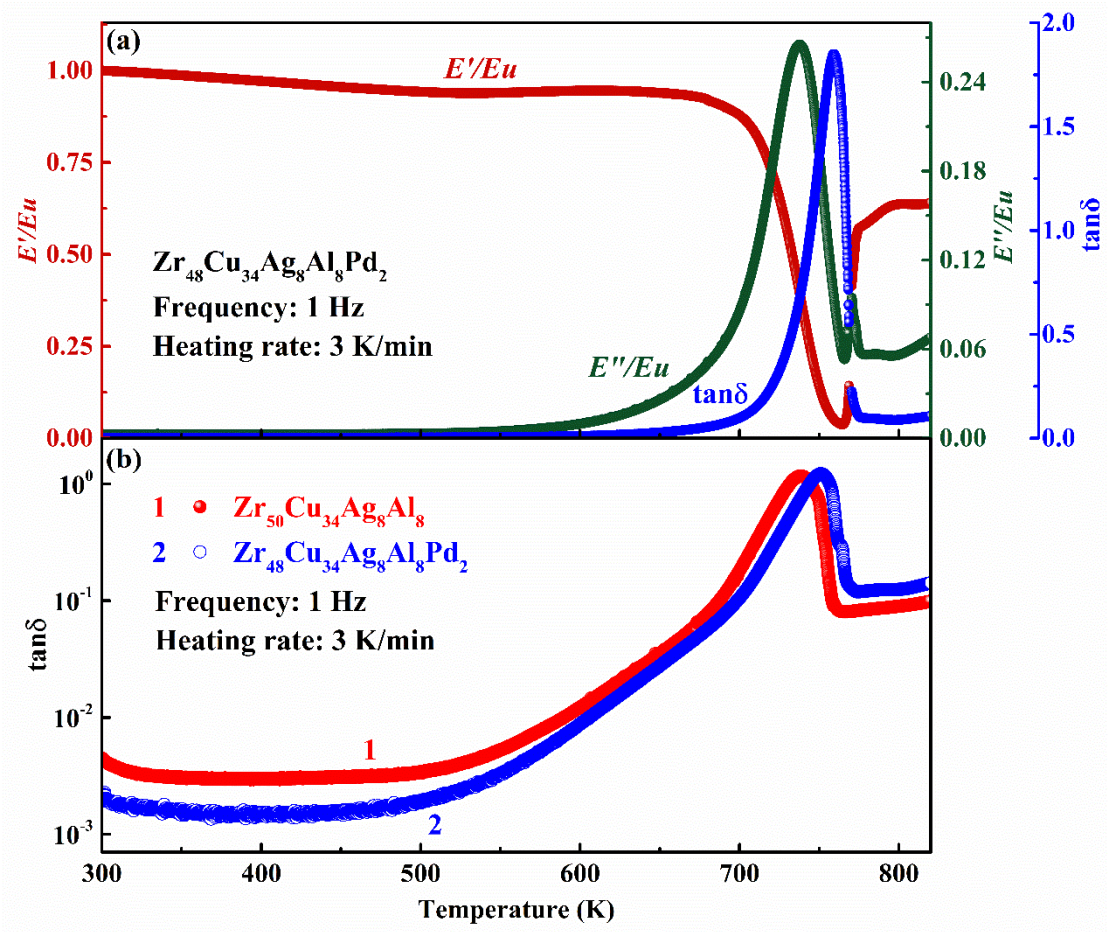

Fig. 2 (a) Temperature dependence of the normalized storage modulus E'/E_u, the normalized loss modulus E''/E_u and the loss factor tan δ for $Zr_{48}Cu_{34}Ag_8Al_8Pd_2$ metallic glass (heating rate: 3 K/min, driving frequency: 1 Hz). E_u is the storage modulus at room temperature. (b) Loss factor tanδ as a function of temperature in $Zr_{50}Cu_{34}Ag_8Al_8$ and $Zr_{48}Cu_{34}Ag_8Al_8Pd_2$ metallic glasses (heating rate: 3 K/min, driving frequency: 1 Hz).

The mechanical relaxation behavior is strongly dependent of the driving frequency of the test. **Fig. 3** shows the evolution of the normalized loss modulus E''/E_u with the temperature of $Zr_{48}Cu_{34}Ag_8Al_8Pd_2$ metallic glass at different frequencies (1 Hz, 2 Hz, 4 Hz and 8 Hz) with a heating rate of 2 K/min. It can be seen that the peak of α relaxation shifts to a higher temperature by increasing the driving frequency. The activation energy E_α of α relaxation can be deduced by the Arrhenius equation:

$$f = f_0 \, exp(-E_\alpha/k_B T) \quad (1)$$

where f indicates the driving frequency, f_0 stands for a pre-exponential factor, k_B is the Boltzmann's constant, E_α is the activation energy of the main relaxation and T is the temperature. The inset of **Fig. 3** shows the variation of the logarithm of frequency ln(f) versus the reciprocal of peak temperature $1/T$, while the solid line is a least-squares fitted curve. According to Eq. (1) and the fitted curve in **Fig. 3**, it can be derived that E_α is equal to 5.855 eV for $Zr_{48}Cu_{34}Ag_8Al_8Pd_2$ metallic glass. By the same method, the activation energy E_α of $Zr_{50}Cu_{34}Ag_8Al_8$ is 5.858 eV. The result is in good agreement with other CuZr-based metallic glass systems[38, 41].This value of the apparent activation energy of the α-relaxation in the super-cooled liquid region corresponds to a liquid fragility of $m = \frac{E_\alpha}{k_B T \ln 10} = 43$.

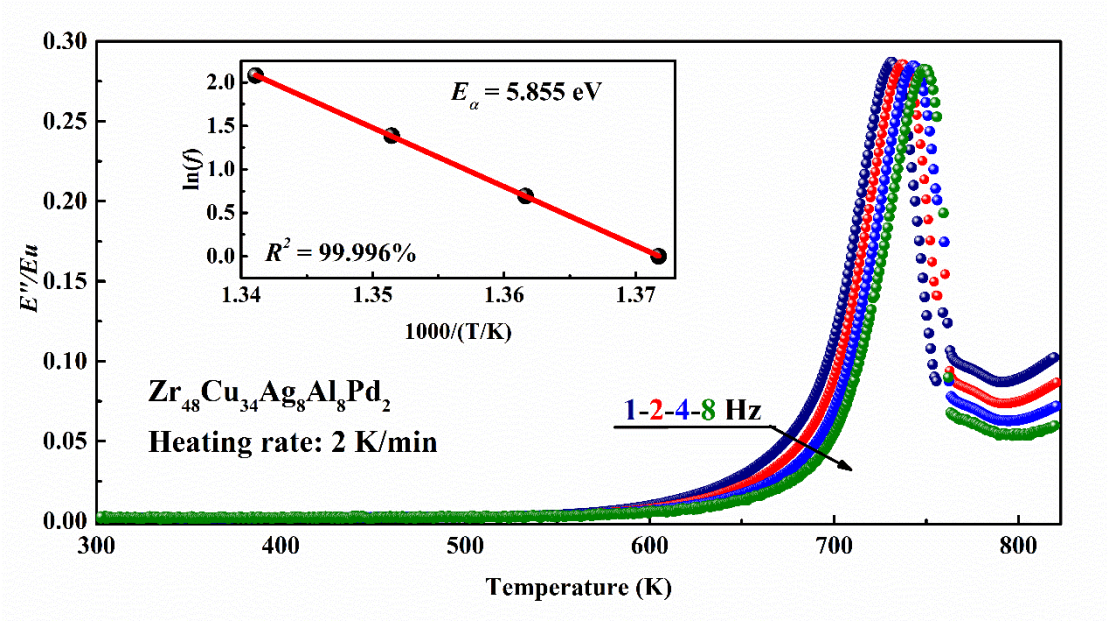

Fig. 3 Temperature dependence of the normalized loss modulus E''/E_u of $Zr_{48}Cu_{34}Ag_8Al_8Pd_2$ metallic glass for different frequencies. The inset shows the relationship between driving frequency and temperature. The solid line is the least-squares fitted curve.

3.2.2. Physical aging analysis

Physical aging below the glass transition temperature was carried out for $Zr_{50}Cu_{34}Ag_8Al_8$ and $Zr_{48}Cu_{34}Ag_8Al_8Pd_2$ metallic glasses. The aging temperatures were

selected with a difference of 9 K between the two alloys, the same difference existing between the two glass transition temperatures. As shown in **Fig. 4**, XRD patterns of samples aged below *Tg* for 18 hours confirm that the amorphous nature of the samples was not changed.

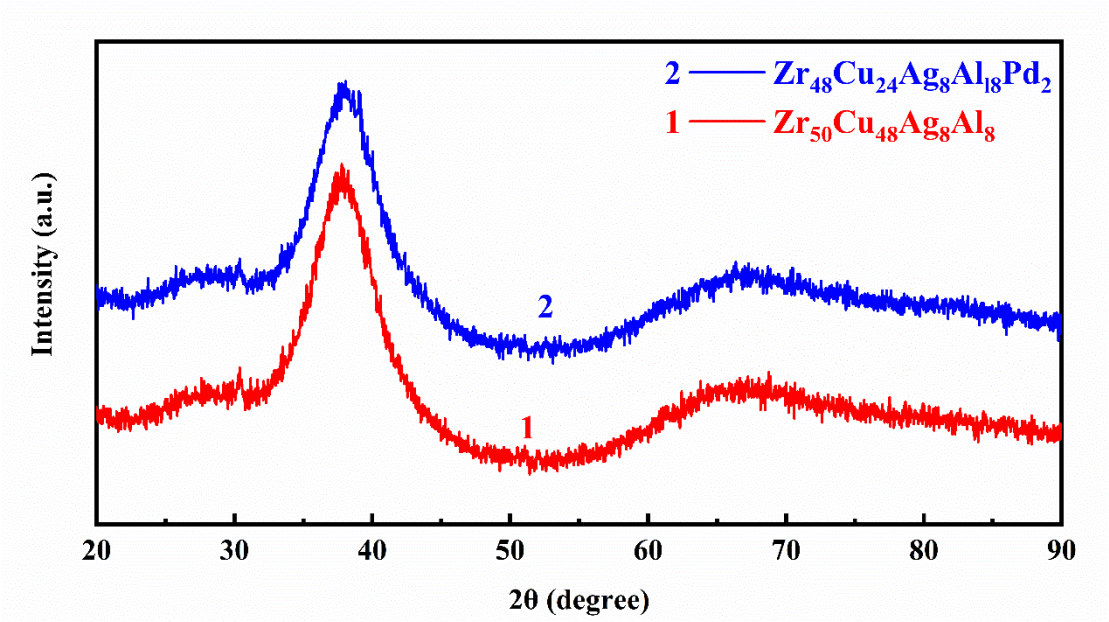

Fig. 4 XRD patterns of $Zr_{48}Cu_{34}Ag_8Al_8Pd_2$ and $Zr_{50}Cu_{34}Ag_8Al_8$ metallic glasses after bein aged at 644.5 K (T_a/T_g = 0.962) and 653 K (T_a/T_g = 0.962) during 18 hours.

Fig. 5 shows the evolution of the normalized storage modulus E'/E_u with aging time of $Zr_{48}Cu_{34}Ag_8Al_8Pd_2$ metallic glass at different annealing temperatures (623 K, 633 K, 643 K and 653 K) and a fixed frequency (1 Hz). The evolution of a given physical/mechanical parameter *P* (like shear modulus, density, enthalpy or hardness) with the aging time can be described in the form of $P_t = \frac{P_\infty}{1+c}$[17, 42]. In the case of the storage modulus, the equation can be expressed as:

$$\frac{E'(t)}{E_u} = \frac{A}{1+c} \tag{2}$$

where *A* is equal to the normalized storage modulus when the aging time approaches infinite. It has been reported that $c = (\frac{\tau_a}{\tau_b+t})^{\beta_c}$ is related to the concentration of flow units, where τ_a, τ_b and β_c are constant at a given temperature[42]. In particular, β_c is related to the velocity of the flow units' annihilation with aging time. According to Eq.

(2), the sensitive parameter β_c for $Zr_{48}Cu_{34}Ag_8Al_8Pd_2$ metallic glass is 0.203, 0.332, 0.385 and 0.468 at annealing temperatures of 623 K, 633 K, 643 K and 653 K, respectively. Clearly, the β_c value increases with annealing temperature, which agrees with the faster annihilation of flow units expected at the higher temperatures.

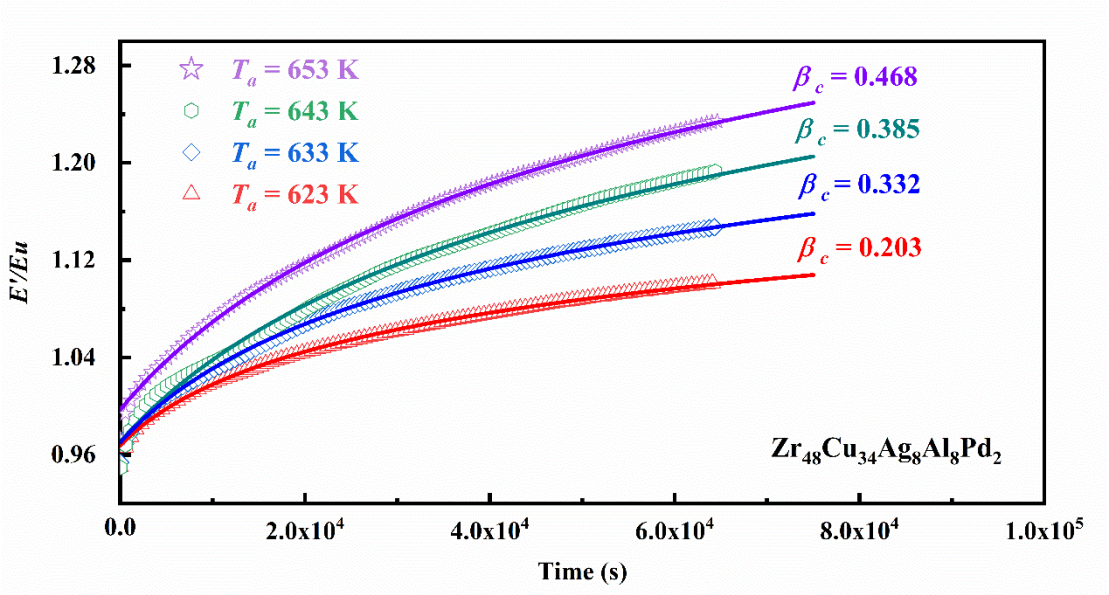

Fig. 5 The normalized storage modulus E'/E_u versus aging time at different annealing temperatures (623 K, 633 K, 643 K and 653 K) in $Zr_{48}Cu_{34}Ag_8Al_8Pd_2$ metallic glass (driving frequency: 1 Hz). The solid lines are the fitted curves using Eq. (2).

Below T_g, metallic glass-forming alloys stay in a non-equilibrium state and physical aging induces the glassy system to shift towards a more stable configuration[12, 43]. Internal friction tanδ of amorphous solids can be described by a Kohlrausch-Williams-Watts (KWW) function[12]:

$$tan\,\delta\,(t_a) - tan\,\delta\,(t_a = 0) = A\{1 - exp[-(t_a/\tau)^{\beta_{aging}}]\} \quad (3)$$

where $A = tan\,\delta\,(t_a \to \infty) - tan\,\delta\,(t_a = 0)$, t_a stands for the aging time and β_{aging} is the Kohlrausch exponent. β_{aging} is between 0 to 1, which reflects the shape of the distribution of timescales underlying the aging process, i.e. the dynamic heterogeneity. $\beta_{aging} = 1$ corresponds to a single Debye relaxation time. Lower β_{aging} reflects a broader distribution of relaxation times and a greater degree of deviation from the Debye relaxation, which is related to a higher dynamic heterogeneity [44].

The evolution of the loss factor tanδ vs aging time at different annealing temperatures for $Zr_{48}Cu_{34}Ag_8Al_8Pd_2$ and $Zr_{50}Cu_{34}Ag_8Al_8$ metallic glasses is illustrated in **Fig. 6**(a) and (b). The driving frequency is 1 Hz. By using Eq. (3) to fit the curves in **Fig. 6**(a) and (b), the β_{aging} values decrease with the increase of annealing temperature for $Zr_{48}Cu_{34}Ag_8Al_8Pd_2$ metallic glass, the same trend of β_{aging} occurs when $T_a > 624.5$ K for $Zr_{50}Cu_{34}Ag_8Al_8$ metallic glass. The β_{aging} decrease with the increase of temperature implies that the dynamic heterogeneity of the metallic glass increases[45]. The dependence of β_{aging} vs annealing temperature in different metallic glasses is not clear. It is expected to be highly dependent on the initial state of the material before the aging experiment and not only on the composition. As illustrated in **Table. 1**, β_{aging} was found around 0.5 in Refs.[46] and [47], while it was found to increase with annealing temperature for $Zr_{50}Cu_{40}Al_{10}$ and $Zr_{58.5}Cu_{15.6}Ni_{12.8}Al_{10.3}Nb_{2.8}$ metallic glasses[48, 49]. In the study of $Zr_{57}Nb_5Al_{10}Cu_{15.4}Ni_{12.6}$, β_{aging} increased with annealing temperature for $T_a/T_g > 0.942$ but did not fluctuate much for $T_a/T_g < 0.942$[50]. In the current work, the decrease of β_{aging} with the increase of annealing temperature accords with the results of $Ti_{36.2}Zr_{30.3}Cu_{8.3}Fe_4Be_{21.2}$ metallic glass[51] .

It is worth noting that β_{aging} values for $Zr_{50}Cu_{34}Ag_8Al_8$ are higher than that of $Zr_{48}Cu_{34}Ag_8Al_8Pd_2$ at the same T_a/T_g (T_a/T_g >0.932). **Fig. 6**(c) shows the loss factor tanδ of $Zr_{50}Cu_{34}Ag_8Al_8$ and $Zr_{48}Cu_{34}Ag_8Al_8Pd_2$ metallic glasses at the same T_a/T_g. The intensity of the loss factor tanδ of $Zr_{50}Cu_{34}Ag_8Al_8$ metallic glass is very similar to that of $Zr_{48}Cu_{34}Ag_8Al_8Pd_2$ metallic glass, only marginally higher in $Zr_{48}Cu_{34}Ag_8Al_8Pd_2$ at $T_a/T_g = 0.962$. In agreement with the analysis using the KWW equation discussed in the following section, it seems the dynamic heterogeneity for the as-cast samples is slightly increased by microalloying.

Chemical composition	T_a/K	T_a/T_g	β_{aging}
$Cu_{46}Zr_{45}Al_7Dy_2$[47]	645	0.935	0.467
	655	0.949	0.455
	665	0.964	0.480

$Zr_{41.2}Ti_{13.8}Cu_{12.5}Ni_{10}Be_{22.5}$[47]	675	0.978	0.471
	600	0.938	0.558
	608	0.950	0.557
	615	0.961	0.558
	625	0.977	0.554
$Ti_{40}Zr_{25}Ni_8Cu_9Be_{18}$[47]	535	0.942	0.533
	540	0.951	0.527
	545	0.960	0.532
	550	0.968	0.548
$Zr_{56}Co_{28}Al_{16}$[46]	675	0.911	0.484
	690	0.931	0.482
	705	0.951	0.486
$Zr_{50}Cu_{40}Al_{10}$[49]	473	0.701	0.65
	573	0.849	0.88
	673	0.997	0.96
$Zr_{58.5}Cu_{15.6}Ni_{12.8}Al_{10.3}Nb_{2.8}$[48]	633	0.959	0.792
	643	0.974	0.799
	653	0.989	0.890
	663	1.00	0.860
$Ti_{36.2}Zr_{30.3}Cu_{8.3}Fe_4Be_{21.2}$[51]	498	0.857	0.421
	523	0.900	0.374
	548	0.943	0.361
	558	0.960	0.355
$Zr_{50}Cu_{34}Ag_8Al_8$ (current work)	615	0.918	0.381
	624.5	0.932	0.457
	634.5	0.947	0.400
	644.5	0.962	0.353
$Zr_{48}Cu_{34}Ag_8Al_8Pd_2$ (current work)	623	0.918	0.405
	633	0.932	0.365
	643	0.947	0.304
	653	0.962	0.254

As shown in **Fig. 5**, the initial value of the storage modulus is very similar and independent on temperature. However, E'/E_u rises with aging time and the change rate increases with annealing temperature. From **Fig. 5**, it is likely that the normalized

storage modulus E'/E_u could reach a stable value if aging time is long enough. In contrast, tanδ decreases with aging time but increases with annealing temperature as presented in **Fig. 6**. Similarly to storage modulus, the loss factor approaches a constant value for very long aging times.

It is generally accepted that metallic glasses are dynamically heterogeneous, composed by regionswith different amounts of free volume or, equivalently, hard and soft regions[52, 53]. Free volume can be considered as a kind of "defects", frozen in the quenched atomic structure [54, 55]. It is conjectured that free volume strongly affects the performance of metallic glasses [55]. Under mechanical probes, softer regions with more free volume enhance the plasticity of metallic glasses[56]. According to Ref. [57], increased structural disorder and lower density correspond to a higher concentration of free volume and vice versa. Rejuvenation, by means of mechanical treatments or other methods like neutron irradiation, can create free volume in the structure, while thermal treatments always reduce free volume [57]. The reduction of free volume decreases the atomic mobility [58], enhances hardness and elastic moduli and induces embrittlement [54, 57, 59]. That is, the atomic mobility characterized by tanδ is reduced by aging, as shown in **Fig. 6**. Due to the relatively fast heating applied to reach the isothermal temperatures of the aging experiments, there is no sufficient structural relaxation during the heating step [57]. Therefore, the normalized storage modulus before aging has approximately the same value at different annealing temperatures (**Fig. 5**). However, the annihilation of free volume occurs during the structural relaxation process, resulting in the evolution of soft regions towards lower energy configurations, i.e. soft regions migrate to hard regions[7], increasing the storage modulus. According to the free volume theory[42], the free volume available in soft regions is primarily reduced and then approaches a characteristic concentration at the given annealing temperature, resulting in constant storage modulus and loss factor. It is observed in **Fig. 5** that even at the highest annealing temperature, the storage modulus is still clearly increasing after more than 60000 s, indicating that the glass is still far from reaching an equilibrated state. It is also interesting to note that due to the much faster aging process, the glasses annealed

at higher temperatures become significantly stiffer than the ones aged at lower temperatures. The free volume content is lower after annealing at higher temperature, which is in agreement with previous works [43, 57].

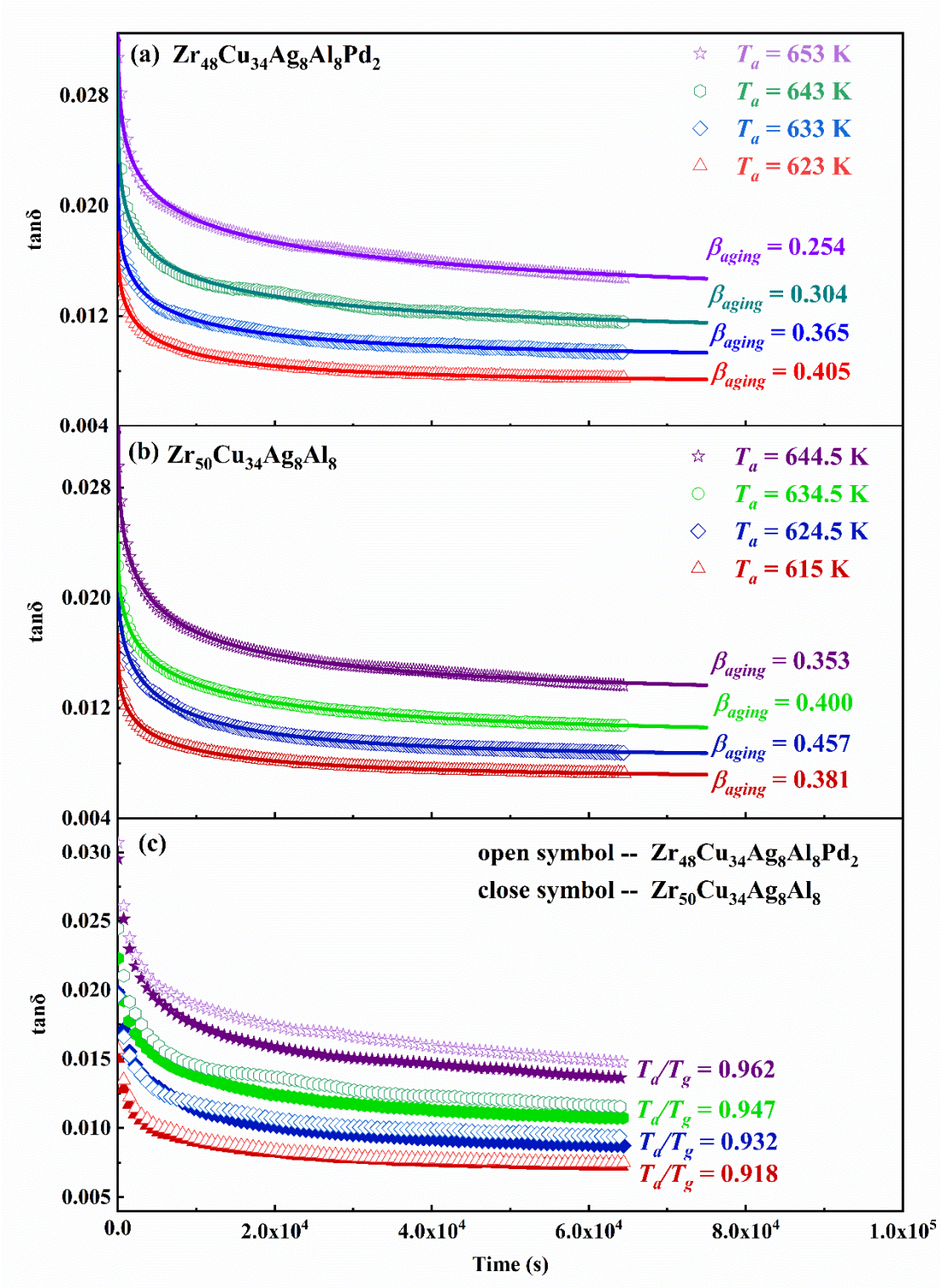

Fig. 6 The loss factor tanδ versus aging time (a) in $Zr_{48}Cu_{34}Ag_8Al_8Pd_2$ metallic glass at different annealing temperatures (623 K, 633 K, 643 K and 653 K) and (b) in

$Zr_{50}Cu_{34}Ag_8Al_8$ metallic glass at different annealing temperatures (615 K, 624.5 K, 634.5 K and 644.5 K). The driving frequency is 1 Hz. The solid lines are fitted curves using Eq. (2). (c) Shows the difference of the loss factor tanδ between $Zr_{50}Cu_{34}Ag_8Al_8$ and $Zr_{48}Cu_{34}Ag_8Al_8Pd_2$ metallic glasses.

3.2.3. Frequency spectrum analysis by Kohlrausch-Williams-Watts (KWW) equation

Isothermal frequency scanning experiments were carried out on $Zr_{50}Cu_{34}Ag_8Al_8$ and $Zr_{48}Cu_{34}Ag_8Al_8Pd_2$ metallic glasses. **Fig. 7**(a) and **Fig. 7**(b) show the evolution of the normalized storage modulus G'/G_u and the normalized loss modulus $G"/G_u$ as a function of frequency for $Zr_{48}Cu_{34}Ag_8Al_8Pd_2$ metallic glass at different temperatures. As displayed in **Fig. 7**(a) and **Fig. 7**(b), the storage modulus decreases by decreasing the driving frequency and increasing temperature. The loss modulus shows a peak at high temperatures, which shifts to lower frequencies as temperature decreases. This peak of $G"/G_u$ corresponds to the α relaxation. According to the time-temperature superposition (TTS) principle[60], master curves of storage modulus and loss modulus of $Zr_{50}Cu_{34}Ag_8Al_8$ and $Zr_{48}Cu_{34}Ag_8Al_8Pd_2$ metallic glasses were drawn and are presented in **Fig. 7**(c) and **Fig. 7**(d), respectively.

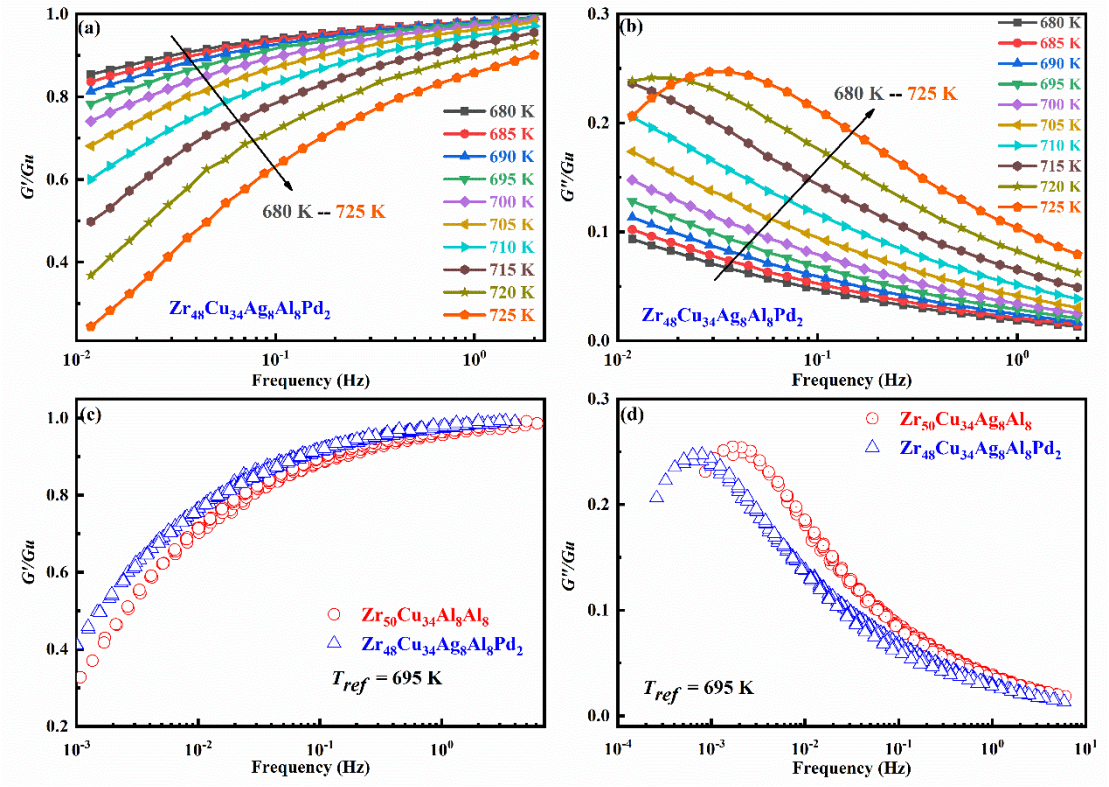

Fig. 7 Variation of (a) the normalized storage modulus G'/G_u and (b) the normalized loss modulus $G"/G_u$ with frequency at different temperatures for $Zr_{48}Cu_{34}Ag_8Al_8Pd_2$ metallic glass. The temperature range is 680 K-725 K and the driving frequency is 0.01-2 Hz. (c) Master curves of the normalized storage modulus of $Zr_{50}Cu_{34}Ag_8Al_8$ and $Zr_{48}Cu_{34}Ag_8Al_8Pd_2$ metallic glasses. (d) Master curves of loss modulus of $Zr_{50}Cu_{34}Ag_8Al_8$ and $Zr_{48}Cu_{34}Ag_8Al_8Pd_2$ metallic glasses.

Williams et al.[61] proposed the use of an empirical dielectric decay function for the analysis of α relaxation:

$$G"(\omega) = \Delta G_\alpha L_{i\omega}[-\frac{d\varphi_\alpha(t,\tau_\alpha)}{dt}]$$

$$\varphi_\alpha(t,\tau_\alpha) = exp[-(t/\tau_\alpha)^{\beta_{KWW}}] \quad (4)$$

where ΔG_α is the relaxation strength, which is equal to the difference between the unrelaxed G_u modulus and the relaxed modulus G_r. $L_{i\omega}$ stands for the Laplace transform, and τ_α is the primary relaxation time. $\varphi_\alpha(t,\ \tau_\alpha)$ is the empirical dielectric decay function mentioned above.

On this basis, Bergman[62] derived the relaxation equation for the glassy material with

only three fitting parameters. As illustrated in **Fig. 8**(a), the α peak of the normalized loss modulus $G"/G_u$ for $Zr_{48}Cu_{34}Ag_8Al_8Pd_2$ metallic glass can be fitted with the following KWW equation:

$$G" = G_P/\left\{1-\beta_{kww}+\frac{\beta_{KWW}}{1+\beta_{KWW}}\left[\beta_{KWW}(\omega_P/\omega)+(\omega/\omega_P)^{\beta_{KWW}}\right]\right\} \quad (5)$$

where β_{KWW} is the Kohlrausch exponent, which ranges from 0 to 1. G_P and ω_p are the normalized loss modulus and frequency at the peak, respectively. According to previous studies, β_{KWW} describes the dynamic inhomogeneity; the larger β_{KWW} the lower the dynamic inhomogeneity[41, 45, 63].

As shown in **Fig. 8**(c), master curves of $Zr_{50}Cu_{34}Ag_8Al_8$ and $Zr_{48}Cu_{34}Ag_8Al_8Pd_2$ metallic glasses can be fitted well by Eq. (5). β_{KWW} values of the master curves for $Zr_{50}Cu_{34}Ag_8Al_8$ and $Zr_{48}Cu_{34}Ag_8Al_8Pd_2$ metallic glasses are 0.503 and 0.490, respectively, which indicates a slight increase in dynamic inhomogeneity by replacing Zr with a small amount of Pd. Master curves are fitted well with Eq. (5) at peaks, while the experimental data shows a deviation from fitting curves in the form of excess wings.

Fig. 8(a) below and previous studies[64] show that the β_{KWW} value rises with the increase of temperature. However, it is worth noting that in the studied temperature range β_{KWW} is quite insensitive to temperature as a master curve with β_{KWW} = 0.5 can be used to describe all the results. The result is in good agreement with the typical β_{KWW} value (0.5) obtained in many metallic glasses[65, 66].

3.2.4. Frequency spectrum analysis by quasi-point defect (QPD) model

The theory of quasi-point defects (QPD) explains the macroscopic dynamic mechanical behavior of glass materials from a microscopic perspective[27, 28]. A physical model was established to quantify the defect concentration. Based on the quasi-point defects theory, $G"/G_u$ can be described by the following equation[67]:

$$G"(i\omega) = G_u/[1+\lambda(i\omega\tau)^{-\chi}+(i\omega\tau)^{-1}] \quad (6)$$

Here λ is a numerical factor, τ is the global characteristic time, and χ is the correlation factor. The values of λ, τ and χ can be obtained by fitting. The correlation factor χ is closely related to the concentration of quasi-point defects, and its value ranges between

0 and 1. χ equal to 0 indicates that the material is a perfect crystal, while χ equal to 1 means that the material is an ideal gas, where the atoms or molecules move independently of their neighbors. **Fig. 8**(d) shows the fitting results of the master curves for $Zr_{50}Cu_{34}Ag_8Al_8$ and $Zr_{48}Cu_{34}Ag_8Al_8Pd_2$ metallic glasses by Eq. (6), showing χ values of 0.419 and 0.406, respectively. It is worth noting that χ decreases as the content of Pd increases, indicating that microalloying reduces the defect concentration and increases the storage modulus (cf. **Fig. 7**(c)). Fitting results show that the excess wing is fitted better by Eq. (6) than by Bergman-KWW equation. It has been proposed in Ref. [68] that the ratio of β_{KWW} and χ is approximately 0.8 for $Cu_{38}Zr_{46}Ag_8Al_8$ metallic glass. For the current work, values of β_{KWW} and χ obtained by master curves follow the same trend, while the ratios of β_{KWW} and χ diverge from 0.8 at higher temperatures, giving ratios of 0.97 at 720 K and 1.05 at 725 K. It may be possible to get a relation between the ratio of β_{KWW} and χ and temperature.

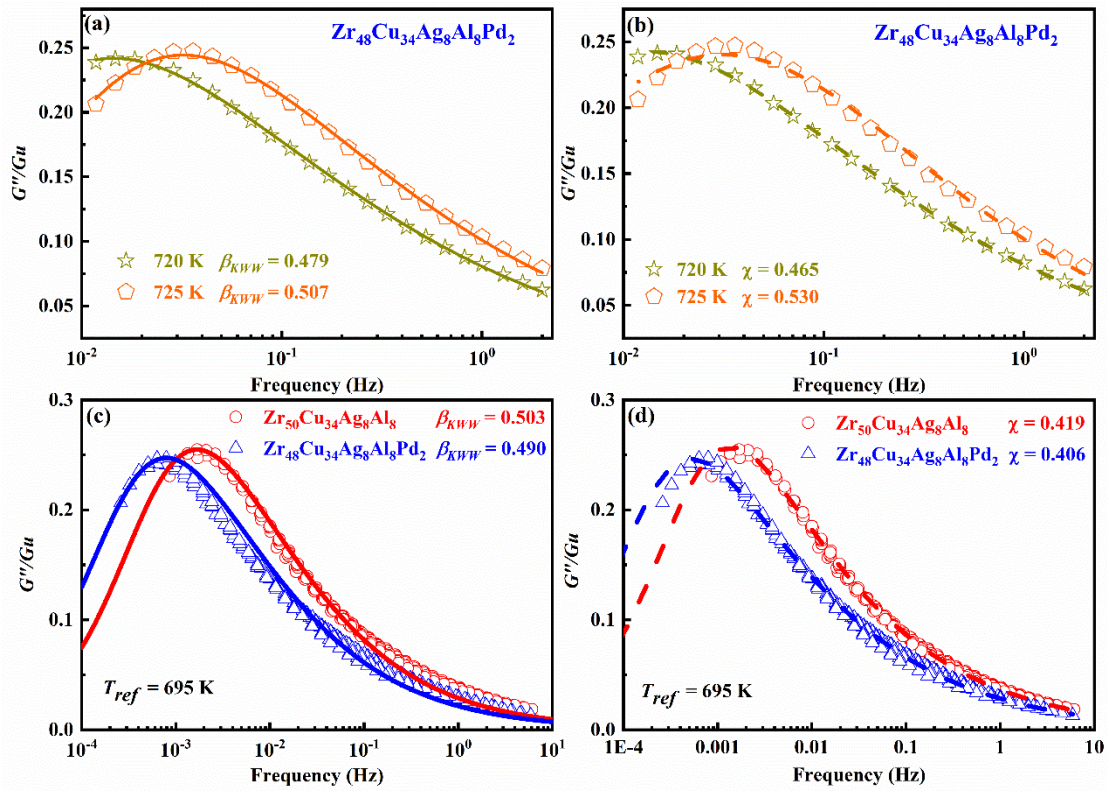

Fig. 8 The fitting result of (a) Eq. (5) and (b) Eq. (6) for the normalized loss modulus G''/G_u of $Zr_{48}Cu_{34}Ag_8Al_8Pd_2$ metallic glasse. Master curves of $Zr_{50}Cu_{34}Ag_8Al_8$ and $Zr_{48}Cu_{34}Ag_8Al_8Pd_2$ metallic glasses fitted by (c) Eq. (5) and (d) Eq. (6)

According to the QPD theory, the loss factor tanδ of the glass can be expressed as[58]:

$$ln(\tan\delta) = -\chi \ln\omega - \chi \ln\tau_r + \ln K_0 - E_\beta/k_B T \quad (7)$$

where τ_r is the characteristic time, K_0 is a scaling factor, E_β is the activation energy of β relaxation and k_B is the Boltzmann constant. The variation of ln(tanδ) with ln(ω) at different temperatures is shown in **Fig. 9**(a), and Eq. (7) gives a good fit for all data. Furthermore, tanδ, which is consistent with viscosity, decreases with the increase of frequency and the decrease of temperature. **Fig. 9**(b) presents the correlation between the values of χ obtained by the fit to Eq. (7) and temperature.

It is remarkable in **Fig. 9**(b) that χ is quite constant below 700 K for the $Zr_{48}Cu_{34}Ag_8Al_8Pd_2$ metallic glass; however, χ increases almost linearly with temperature above 700 K. The result is in agreement with reported discussions and the prediction of QPD theory[41, 46, 58]. On the basis of the QPD theory, when temperature is lower than T_g, the concentration of defects in the metallic glass remains almost constant and the atomic movement is restricted. When the temperature rises above T_g, more atoms are activated resulting in an increase in defect concentration.

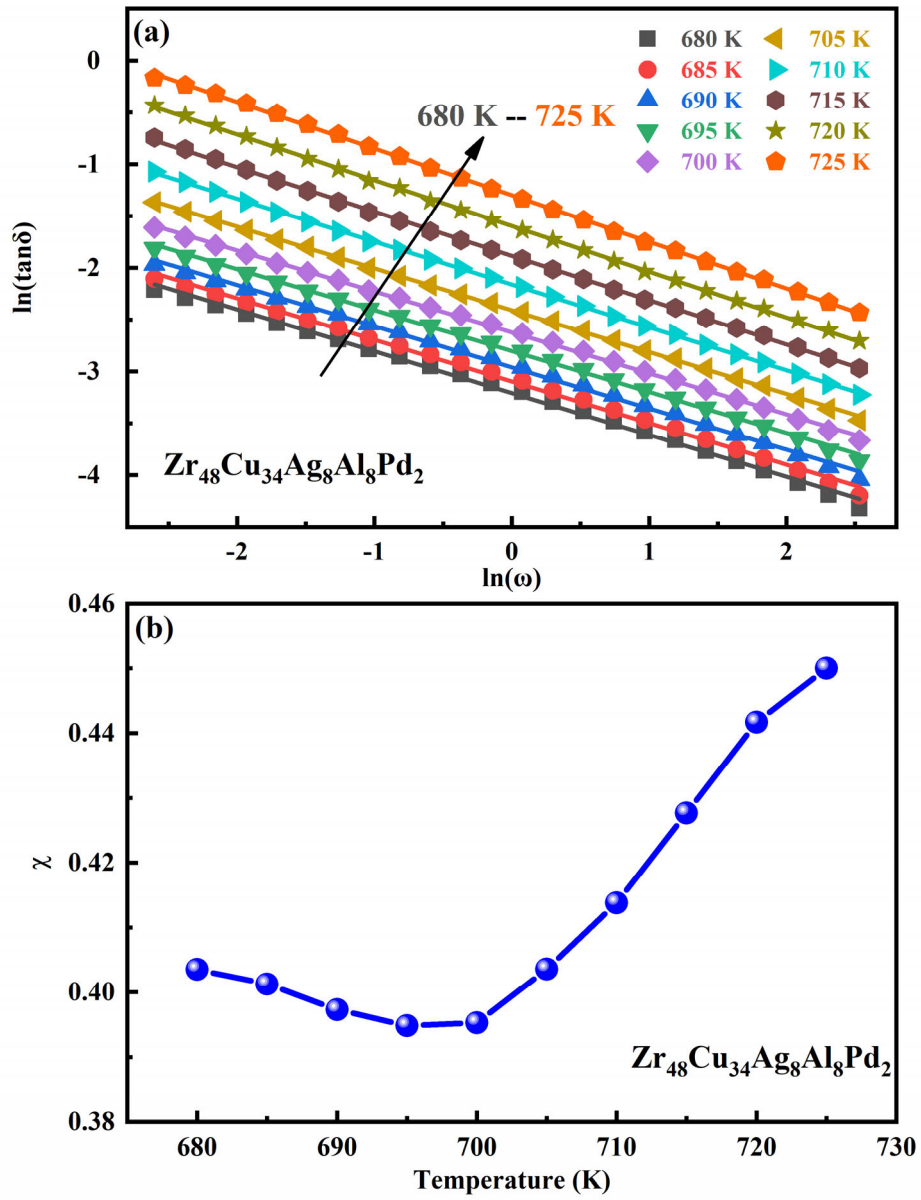

Fig. 9 (a) Influence of the driving frequency on the loss factor tanδ at various temperatures of $Zr_{48}Cu_{34}Ag_8Al_8Pd_2$ metallic glass (the isothermal temperatures range from 680 to 725 K with an interval of 5 K). Solid lines correspond to the fit to Eq. (7). (b) The correlation factor χ as a function of temperature of the $Zr_{48}Cu_{34}Ag_8Al_8Pd_2$ metallic glass.

3.2.5. Frequency spectrum analysis by Havriliak-Negami (HN) function

The validity of the TTS principle demonstrated above by the construction of the master curves allows us to determine the temperature dependence of the relaxation times by fitting the frequency response to a Havriliak-Negami (HN) function.

$$G^*(\omega) = \frac{\Delta G}{(1+(i\omega\tau)^{\xi})^{\gamma}} \quad (8)$$

The empirical frequency-domain HN and time-domain KWW functions represent the same underlying relaxation time spectrum for given values of the ξ, γ and β_{KWW} exponents as detailed in ref.[69]. ΔG is the relaxation strength. As shown in **Fig. 10**(a), the experimental data of the isothermal experiments can be well fitted by HN functions with $\xi = 0.8091$ and $\gamma = 0.5105$ corresponding to a $\beta_{KWW} = 0.5$ as already obtained above from Eq. (5). **Fig. 10**(b) presents the best fitted results by Eq. (8), which exhibits the excellent ability to describe the main relaxation. This is in agreement with the results in many other metallic glass systems[64] and it is a further evidence that most metallic glasses show a remarkable similarity in terms of the underlying relaxation spectrum of the α relaxation.

The relaxation times obtained from the HN fitting are shown in **Figs. 10**(c) and (d). It is observed that the relaxation time behavior as a function of temperature shows the change in slope expected in the glass transition region, which is the temperature window explored by the isothermal measurements analyzed here. It is interesting to note that the addition of Pd shifts the response of the system towards higher temperatures, but it does not significantly alter neither the relaxation time distribution shape nor the apparent activation energies of the α-relaxation both in the liquid and the glass state. This fact is clearly shown by the superposition of the relaxation times as a function of T_g^*/T, with T_g^* chosen as the temperature at which the HN relaxation time is 100 s.

As presented in **Fig. 10**(c), the relaxation time falls with the rise of temperature, as expected due to the faster rearrangement of atoms at higher temperatures. The fragility parameter *m* is an important indicator in amorphous materials, which is used to evaluate the deviation from Arrhenius equation[70]. According to **Fig. 10**(d), the fragility parameter of $Zr_{48}Cu_{34}Ag_8Al_8Pd_2$ metallic glass is identical to the Pd-free alloy.

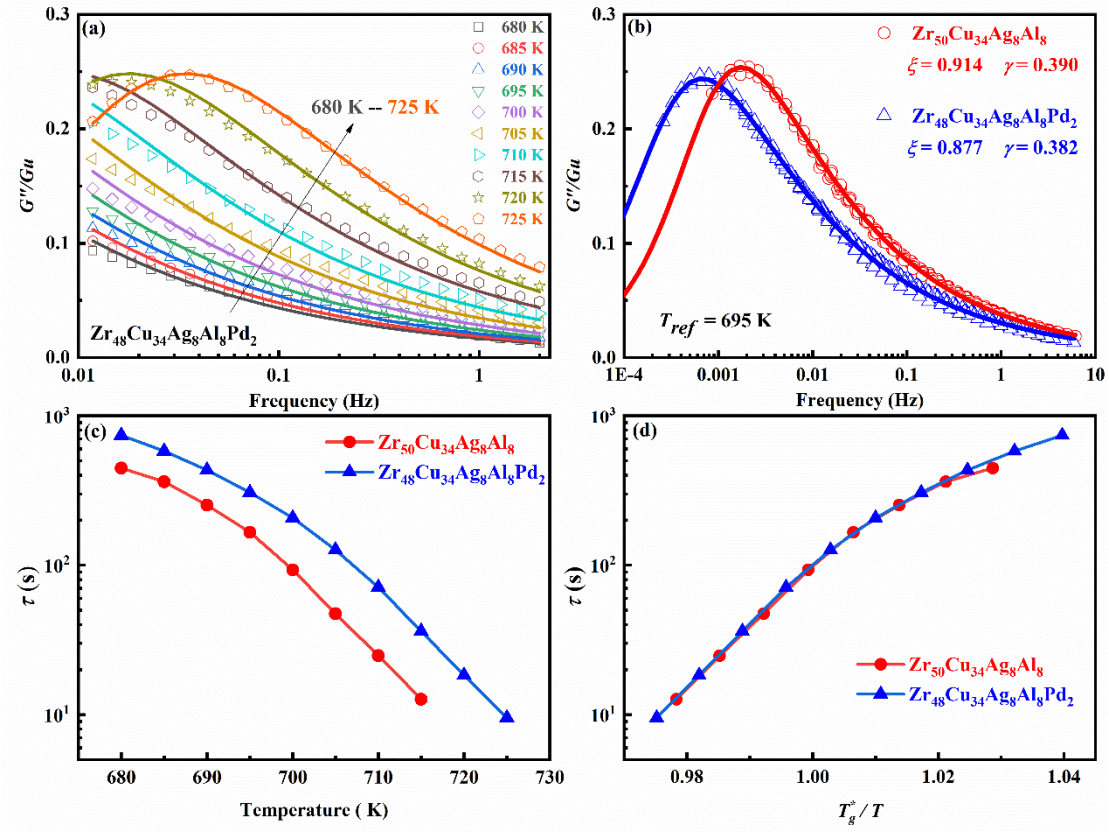

Fig. 10 (a) Isothermal $G^*(\omega)$ measurements and the corresponding HN fitted functions for $Zr_{48}Cu_{34}Ag_8Al_8Pd_2$ metallic glass. (b) Master curves fitted by HN model for $Zr_{50}Cu_{34}Ag_8Al_8$ and $Zr_{48}Cu_{34}Ag_8Al_8Pd_2$ metallic glasses. (c) HN relaxation times as function of temperature and (d) as function of T_g^*/T for $Zr_{50}Cu_{34}Ag_8Al_8$ and $Zr_{48}Cu_{34}Ag_8Al_8Pd_2$ metallic glasses.

4. Conclusions

The dynamic mechanical response of $Zr_{50}Cu_{34}Ag_8Al_8$ and $Zr_{48}Cu_{34}Ag_8Al_8Pd_2$ metallic glasses was analyzed in the temperature range of the glass transition temperature. The microalloying effect due to the replacement of 2% of Zr by Pd substantially affects the atomic mobility. Both the glass transition temperature and the mechanical response are affected, in a consistent way.

Quantification of the different glass dynamics was performed by analyzing the aging through the formula $P_t = \frac{P_\infty}{1+c}$, and the relaxation spectrum using the KWW equation, the QPD theory and the HN model. $P_t = \frac{P_\infty}{1+c}$ is efficient to describe the aging

process and parameter β_c reflects the velocity of the flow units' annihilation with aging time. The KWW is a widely used fitting model that can fit proper the annealing and primary relaxation kinetics. The QPD model properly fits the primary relaxation and allows us to determine the defect concentration evolution with temperature. The effect of Pd on the relaxation time is analyzed by the HN model. The combined study of the glass dynamics with the KWW and QPD models allowed us to get an insight on the origin of dynamic inhomogeneity.

The β_c value increases with the rise of temperature, which is in agreement with more intense rearrangement in atoms and molecules. The validity of the time temperature superposition in the studied temperature range is confirmed, and master curves were computed for both alloys. The master curve of the loss modulus of the Pd-containing alloy shifts to lower frequencies, coherently with the increase of the glass transition temperature.

Both the KWW model and the QPD model describe properly the effect of temperature in the dynamics of the glass along the glass transition. The correlation factor χ related to the concentration of quasi-point defects shows a nearly constant value in the glass. Above the glass transition, the β_{KWW} exponent slightly increases with temperature, denoting a small decrease of the dynamic heterogeneity, while the correlation factor χ which describes the concentration of quasi-point defects increases as the glass evolves towards the liquid state. According to the analysis of the HN model, the relaxation time distribution shape and the apparent activation energies of the α-relaxation are not significantly altered by the addition of Pd both in the liquid and the glass state. The time-temperature superposition principle allows us to determine the characteristic relaxation times of both glasses, which confirm the shifting of the dynamics of the glass towards higher temperatures by the minor replacement of Zr by Pd.

Summarizing, this work shows how the atomic dynamics and thermal properties of metallic glasses can be tailored through microalloying by fully characterizing the effect of Pd addition in a $Zr_{50}Cu_{34}Ag_8Al_8$ metallic glass.

Acknowledgements

This work is supported by the NSFC (Grant No. 51971178), the research of JCQ was supported by the Fundamental Research Funds for the Central Universities (Grant Nos. 3102019ghxm007 and 3102017JC01003), Astronautics Supporting Technology Foundation of China (Grant No.2019-HT-XG), the Natural Science Foundation of Shaanxi Province (Grant No. 2019JM-344). E. Pineda and D. Crespo acknowledge financial support from MICINN (grant FIS2017-82625-P) and Generalitat de Catalunya (grant 2017SGR0042).

References

[1] A. Inoue, B.L. Shen, H. Koshiba, H. Kato, A.R. Yavari, Ultra-high strength above 5000 MPa and soft magnetic properties of Co–Fe–Ta–B bulk glassy alloys, Acta Mater. 52 (2004) 1631-1637.

[2] S.H. Chang, S.K. Wu, Textures in cold-rolled and annealed Ti50Ni50 shape memory alloy, Scripta Mater. 50 (2004) 937-941.

[3] R.D. Conner, R.B. Dandliker, V. Scruggs, W.L. Johnson, Dynamic deformation behavior of tungsten-fiber/metallic–glass matrix composites, Int. J. Impact Eng. 24 (2000) 435-444.

[4] Z.L. Long, C.T. Chang, Y.H. Ding, Y. Shao, P. Zhang, B.L. Shen, A. Inoue, Corrosion behavior of Fe-based ferromagnetic (Fe, Ni)-B-Si-Nb bulk glassy alloys in aqueous electrolytes, J. Non-Cryst. Solids 354 (2008) 4609-4613.

[5] A. Inoue, Amorphous, nanoquasicrystalline and nanocrystalline alloys in Al-based systems, Prog. Mater Sci. 43 (1998) 365-520.

[6] A. Inoue, Stabilization of metallic supercooled liquid and bulk amorphous alloys, Acta Mater. 48 (2000) 279-306.

[7] W.H. Wang, Dynamic relaxations and relaxation-property relationships in metallic glasses, Prog. Mater Sci. 106 (2019).

[8] A. Inoue, A. Takeuchi, Recent development and application products of bulk glassy alloys, Acta Mater. 59 (2011) 2243-2267.

[9] M.A. Gibson, N. Mykulowycz, J.Y. Shim, R.R. Fontana, P.A. Schmitt, A. Roberts, J. Ketkaew, L. Shao, W. Chen, P. Bordeenithikasem, 3D printing metals like thermoplastics: Fused filament fabrication of metallic glasses, Mater. Today 21 (2018) 697-702.

[10] P.G. Debenedetti, F.H. Stillinger, Supercooled Liquids and the Glass Transition, Nature 410 (2001) 259-267.

[11] H.-B. Yu, W.-H. Wang, K. Samwer, The β relaxation in metallic glasses: an overview, Mater. Today 16 (2013) 183-191.

[12] J.C. Qiao, J.M. Pelletier, Dynamic Mechanical Relaxation in Bulk Metallic

Glasses: A Review, J. Mater. Sci. Technol. 30 (2014) 523-545.
[13] C. Liu, E. Pineda, D. Crespo, Mechanical Relaxation of Metallic Glasses: An Overview of Experimental Data and Theoretical Models, Metals 5 (2015) 1073-1111.
[14] K.L. Ngai, Relaxation and Diffusion in Complex Systems, Springer, New York, 2011.
[15] J.C. Qiao, Q. Wang, D. Crespo, Y. Yang, J.M. Pelletier, Amorphous physics and materials: Secondary relaxation and dynamic heterogeneity in metallic glasses: A brief review, Chin. Phys. B 26 (2017).
[16] Q. Wang, J.J. Liu, Y.F. Ye, T.T. Liu, S. Wang, C.T. Liu, J. Lu, Y. Yang, Universal secondary relaxation and unusual brittle-to-ductile transition in metallic glasses, Mater. Today 20 (2017) 293-300.
[17] J.C. Qiao, Q. Wang, J.M. Pelletier, H. Kato, R. Casalini, D. Crespo, E. Pineda, Y. Yao, Y. Yang, Structural heterogeneities and mechanical behavior of amorphous alloys, Prog. Mater Sci. 104 (2019) 250-329.
[18] H.B. Yu, X. Shen, Z. Wang, L. Gu, W.H. Wang, H.Y. Bai, Tensile Plasticity in Metallic Glasses with Pronounced beta Relaxations, Phys. Rev. Lett. 108 (2012) 1-5.
[19] Z. Wang, W.-H. Wang, Flow units as dynamic defects in metallic glassy materials, Natl. Sci. Rev. 6 (2019) 304-323.
[20] G.P. Johari, Source of JG-Relaxation in the Entropy of Glass, J. Phys. Chem. B 123 (2019) 3010-3023.
[21] E. Pineda, P. Bruna, B. Ruta, M. Gonzalez-Silveira, D. Crespo, Relaxation of rapidly quenched metallic glasses: Effect of the relaxation state on the slow low temperature dynamics, Acta Materialia 61 (2013) 3002-3011.
[22] Z.G. Zhu, Y.Z. Li, Z. Wang, X.Q. Gao, P. Wen, H.Y. Bai, K.L. Ngai, W.H. Wang, Compositional origin of unusual beta-relaxation properties in La-Ni-Al metallic glasses, J. Chem. Phys. 141 (2014) 1-12.
[23] T. Perez-Castaneda, C. Rodriguez-Tinoco, J. Rodriguez-Viejo, M.A. Ramos, Suppression of tunneling two-level systems in ultrastable glasses of indomethacin, Proc. Natl. Acad. Sci. U.S.A. 111 (2014) 11275-11280.
[24] J. Qiao, J.M. Pelletier, R. Casalini, Relaxation of bulk metallic glasses studied by mechanical spectroscopy, J. Phys. Chem. B 117 (2013) 13658-13666.
[25] P. Rösner, K. Samwer, P. Lunkenheimer, Indications for an “excess wing” in metallic glasses from the mechanical loss modulus in Zr65Al7.5Cu27.5, Europhys. Lett. 68 (2004) 226-232.
[26] D. Turnbull, M.H. Cohen, Free‐Volume Model of the Amorphous Phase: Glass Transition, J. Chem. Phys. 34 (1961) 120-125.
[27] J. Perez, Defect diffusion model for volume and enthalpy recovery in amorphous polymers, Polymer 29 (1988) 483-489.
[28] J. Perez, Quasi-punctual defects in vitreous solids and liquid-glass transition, Solid State Ion. 39 (1990) 69-79.
[29] Y.H. Liu, G. Wang, R.J. Wang, D.Q. Zhao, M.X. Pan, W.H. Wang, Super plastic bulk metallic glasses at room temperature, Science 315 (2007) 1385-1388.
[30] M.Q. Jiang, L.H. Dai, Short-range-order effects on intrinsic plasticity of metallic glasses, Philos. Mag. Lett. 90 (2010) 269-277.

[31] J.C. Qiao, J.M. Pelletier, H.C. Kou, X. Zhou, Modification of atomic mobility in a Ti-based bulk metallic glass by plastic deformation or thermal annealing, Intermetallics 28 (2012) 128-137.
[32] H.B. Yu, K. Samwer, W.H. Wang, H.Y. Bai, Chemical influence on beta-relaxations and the formation of molecule-like metallic glasses, Nat. Commun. 4 (2013) 2204.
[33] J.C. Qiao, Y. Yao, J.M. Pelletier, L.M. Keer, Understanding of micro-alloying on plasticity in Cu 46 Zr 47-x Al 7 Dy x (0≤ x ≤ 8) bulk metallic glasses under compression: Based on mechanical relaxations and theoretical analysis, Int. J. Plast. 82 (2016) 62-75.
[34] G.R. Garrett, M.D. Demetriou, J. Chen, W.L. Johnson, Effect of microalloying on the toughness of metallic glasses, Appl. Phys. Lett. 101 (2012).
[35] W.-j. Peng, Y. Zhang, Micro-alloying of yttrium in Zr-based bulk metallic glasses, Prog. Nat. Sci. 21 (2011) 46-52.
[36] S.M. Chathoth, B. Damaschke, J.P. Embs, K. Samwer, Giant changes in atomic dynamics on microalloying metallic melt, Appl. Phys. Lett. 95 (2009).
[37] S. Etienne, J.Y. Cavaille, J. Perez, R. Point, M. Salvia, Automatic system for analysis of micromechanical properties, Rev. Sci. Instrum. 53 (1982) 1261-1266.
[38] J.C. Qiao, Y.X. Chen, J.M. Pelletier, H. Kato, D. Crespo, Y. Yao, V.A. Khonik, Viscoelasticity of Cu- and La-based bulk metallic glasses: Interpretation based on the quasi-point defects theory, Mater. Sci. Eng., A 719 (2018) 164-170.
[39] J.C. Qiao, J.M. Pelletier, Dynamic mechanical analysis in La-based bulk metallic glasses: Secondary (beta) and main (alpha) relaxations, J. Appl. Phys. 112 (2012) 1-6.
[40] W. Zhang, Q. Zhang, A. Inoue, Synthesis and Mechanical Properties of New Cu-Zr-based Glassy Alloys with high Glass-Forming Ability, Adv. Eng. Mater. 10 (2008) 1034-1038.
[41] G.J. Lyu, J.C. Qiao, J.M. Pelletier, Y. Yao, The dynamic mechanical characteristics of Zr-based bulk metallic glasses and composites, Mater. Sci. Eng., A 711 (2018) 356-363.
[42] D.P. Wang, Z.G. Zhu, R.J. Xue, D.W. Ding, H.Y. Bai, W.H. Wang, Structural perspectives on the elastic and mechanical properties of metallic glasses, J. Appl. Phys. 114 (2013).
[43] J.C. Qiao, J.M. Pelletier, Influence of thermal treatments and plastic deformation on the atomic mobility in Zr50.7Cu28Ni9Al12.3 bulk metallic glass, J. Alloys Compd. 615 (2014) S85-S89.
[44] G. Lyu, J. Qiao, J. Gu, M. Song, J.-M. Pelletier, Y. Yao, Experimental analysis to the structural relaxation of Ti48Zr20V12Cu5Be15 metallic glass matrix composite, J. Alloys Compd. 769 (2018) 443-452.
[45] Z. Wang, B.A. Sun, H.Y. Bai, W.H. Wang, Evolution of hidden localized flow during glass-to-liquid transition in metallic glass, Nat Commun 5 (2014) 5823.
[46] J.C. Qiao, J.M. Pelletier, C. Esnouf, Y. Liu, H. Kato, Impact of the structural state on the mechanical properties in a Zr－Co－Al bulk metallic glass, J. Alloys Compd. 607 (2014) 139-149.

[47] J.C. Qiao, J.M. Pelletier, Kinetics of structural relaxation in bulk metallic glasses by mechanical spectroscopy: Determination of the stretching parameter βKWW, Intermetallics 28 (2012) 40-44.
[48] I. Gallino, M.B. Shah, R. Busch, Enthalpy relaxation and its relation to the thermodynamics and crystallization of the Zr58.5Cu15.6Ni12.8Al10.3Nb2.8 bulk metallic glass-forming alloy, Acta Mater. 55 (2007) 1367-1376.
[49] A. Ishii, F. Hori, A. Iwase, Y. Yokoyama, T.J. Konno, Free Volume Relaxation Process in Zr50Cu40Al10 Bulk Metallic Glass Studied by Positron Annihilation Techniques, Mrs Online Proceeding Library Archive 1048 (2007) 1048-Z08-19.
[50] Y.J. Duan, D.S. Yang, J.C. Qiao, D. Crespo, J.M. Pelletier, L. Li, K. Gao, T. Zhang, Relaxation of internal friction and shear viscosity in Zr57Nb5Al10Cu15.4Ni12.6 metallic glass, Intermetallics 124 (2020).
[51] J.C. Qiao, Y.H. Chen, G.J. Lyu, K.K. Song, J.M. Pelletier, Y. Yao, Mechanical Relaxation of a Ti36.2Zr30.3Cu8.3Fe4Be21.2 Bulk Metallic Glass: Experiments and Theoretical Analysis, Acta Metall. Sin.-Engl. Lett. 32 (2019) 726-732.
[52] C. Zhang, J.C. Qiao, J.M. Pelletier, Y. Yao, Bulk metallic glasses: “Defects” determines performance, Mater. Sci. Eng., A 675 (2016) 379-385.
[53] T. Ichitsubo, E. Matsubara, T. Yamamoto, H.S. Chen, N. Nishiyama, J. Saida, K. Anazawa, Microstructure of fragile metallic glasses inferred from ultrasound-accelerated crystallization in Pd-based metallic glasses, Phys. Rev. Lett. 95 (2005) 245501.
[54] Y.P. Mitrofanov, D.P. Wang, A.S. Makarov, W.H. Wang, V.A. Khonik, Towards understanding of heat effects in metallic glasses on the basis of macroscopic shear elasticity, Sci Rep 6 (2016) 23026.
[55] X. Tong, G. Wang, Z.H. Stachurski, J. Bednarcik, N. Mattern, Q.J. Zhai, J. Eckert, Structural evolution and strength change of a metallic glass at different temperatures, Sci Rep 6 (2016) 30876.
[56] L.Y. Chen, A.D. Setyawan, H. Kato, A. Inoue, G.Q. Zhang, J. Saida, X.D. Wang, Q.P. Cao, J.Z. Jiang, Free-volume-induced enhancement of plasticity in a monolithic bulk metallic glass at room temperature, Scripta Mater. 59 (2008) 75-78.
[57] J. Brechtl, H. Wang, N.A.P.K. Kumar, T. Yang, Y.R. Lin, H. Bei, J. Neuefeind, W. Dmowski, S.J. Zinkle, Investigation of the thermal and neutron irradiation response of BAM-11 bulk metallic glass, J. Nucl. Mater. 526 (2019).
[58] J.-M. Pelletier, D.V. Louzguine-Luzgin, S. Li, A. Inoue, Elastic and viscoelastic properties of glassy, quasicrystalline and crystalline phases in Zr65Cu5Ni10Al7.5Pd12.5 alloys, Acta Mater. 59 (2011) 2797-2806.
[59] Q. Hao, J.-C. Qiao, E.V. Goncharova, G.V. Afonin, M.-N. Liu, Y.-T. Cheng, V.A. Khonik, Thermal effects and evolution of the defect concentration based on shear modulus relaxation data in a Zr-based metallic glass, Chin. Phys. B 29 (2020).
[60] W.M. Jones, Viscoelastic Properties of Polymers : by J.D. Ferry, John Wiley and Son, 1980, 3rd Edition, J. Non-Newton. Fluid Mech. 8 (1981).
[61] G. Williams, D.C. Watts, Non-symmetrical dielectric relaxation behaviour arising from a simple empirical decay function, Trans. Faraday Society 66 (1970).
[62] R. Bergman, General susceptibility functions for relaxations in disordered

systems, J. Appl. Phys. 88 (2000) 1356-1365.
[63] Z.R. Xu, D.S. Yang, J.C. Qiao, J.M. Pelletier, D. Crespo, E. Pineda, Y.-J. Wang, Unified perspective on structural heterogeneity of a LaCe-based metallic glass from versatile dynamic stimuli, Intermetallics 125 (2020).
[64] Z.F. Yao, J.C. Qiao, J.M. Pelletier, Y. Yao, Characterization and modeling of dynamic relaxation of a Zr-based bulk metallic glass, J. Alloys Compd. 690 (2017) 212-220.
[65] L.M. Wang, R. Liu, W.H. Wang, Relaxation time dispersions in glass forming metallic liquids and glasses, J. Chem. Phys. 128 (2008) 164503.
[66] J.C. Qiao, J.M. Pelletier, Mechanical relaxation in a Zr-based bulk metallic glass: Analysis based on physical models, J. Appl. Phys. 112 (2012).
[67] J.M. Pelletier, B.V.d. Moortèle, I.R. Lu, Viscoelasticity and viscosity of Pd－Ni－Cu－P bulk metallic glasses, Mater. Sci. Eng., A 336 (2002) 190-195.
[68] J.C. Qiao, J.M. Pelletier, Dynamic universal characteristic of the main (α) relaxation in bulk metallic glasses, J. Alloys Compd. 589 (2014) 263-270.
[69] F. Alvarez, A. Alegra, J. Colmenero, Relationship between the time-domain Kohlrausch-Williams-Watts and frequency-domain Havriliak-Negami relaxation functions, Phys. Rev. B 44 (1991) 7306-7312.
[70] J.C. Qiao, J.M. Pelletier, Q. Wang, W. Jiao, W.H. Wang, On calorimetric study of the fragility in bulk metallic glasses with low glass transition temperature: (Ce0.72Cu0.28)90−x Al10Fex (x = 0, 5 or 10) and Zn38Mg12Ca32Yb18, Intermetallics 19 (2011) 1367-1373.